PHOTOS Monte Carlo: a precision tool for QED corrections in Z and W decays

P. Golonka[1,2,a], Z. Was[1,2,b]

[1] CERN, 1211 Geneva 23, Switzerland
[2] Institute of Nuclear Physics, ul. Radzikowskiego 152, 31-342 Kraków, Poland

Abstract. We present a discussion of the precision for the PHOTOS Monte Carlo algorithm, with improved implementation of QED interference and multiple-photon radiation. The main application of PHOTOS is the generation of QED radiative corrections in decays of any resonances, simulated by a "host" Monte Carlo generator. By careful comparisons automated with the help of the MC-TESTER tool specially tailored for that purpose, we found that the precision of the current version of PHOTOS is of 0.1% in the case of Z and W decays. In the general case, the precision of PHOTOS was also improved, but this will not be quantified here.

1 Introduction

In the analysis of data from high-energy physics experiments, one tries to resolve the "*experiment = theory*" equation. This non-trivial task requires that a lot of different effects be considered simultaneously. From the experimental side, these are mainly detector acceptance and cuts, which are dictated by the construction and physical properties of the detector: the shapes of distributions may be distorted by, say, misidentification and residual background contamination; these effects need to be discriminated in an appropriate and well-controlled way. From the theoretical side, *all* effects of known physics have to be included in predictions as well. Only then can experimental data and theoretical predictions be confronted to determine numerical values of some coupling constants or effects of new physics (to be discovered).

A well-defined class of theoretical effects consists of QED radiative corrections. PHOTOS is a universal Monte Carlo algorithm that simulates the effects of QED radiative corrections in decays of particles and resonances. It is a project with a rather long history: the first version was released in 1991 [1], followed by version 2.0 [2] (double emission, threshold terms for fermions). The package is in wide use [3]; recently it was applied as a precision simulation tool for W mass measurement at the Tevatron [4] and LEP [5,6], and for CKM matrix measurements in decays of K and B resonances (NA48 [7], KTeV [8], Belle [9], BaBar [10] and in Fermilab [11]).

^{a} e-mail: Piotr.Golonka@cern.ch
^{b} Supported in part by the EU grant MTKD-CT-2004-510126, in partnership with the CERN Physics department, and Polish State Committee for Scientific Research (KBN) grant 2 P03B 091 27 for the years 2004–2006

Throughout the years the core algorithm for the generation of $O(\alpha)$ corrections did not change much; however, its precision, applicability to various processes, and numerical stability improved significantly. Increased interest in the algorithm expressed by experimental collaborations (including future LHC experiments) was a motivation to perform a more detailed study of the potential and precision of the PHOTOS algorithm; also new functionalities, such as multiple photon radiation and better interference corrections, were recently introduced. The main purpose of this paper is however not to document the new features of PHOTOS, as this will be done elsewhere [12,13], but rather to present the results of precision tests of the algorithm.

Our paper is organized as follows. In Sect. 2 we present the physical problem and further motivation for our studies. In Sect. 3 we recapitulate the properties of the PHOTOS algorithm. In Sect. 4 we present the testing procedure and necessary tools we employed to obtain our main results, which are presented in Sect. 5. Finally, Sect. 6 summarizes the paper and gives an outlook to further developments. In the appendix we describe the most important features of the new version of the PHOTOS code. Because of its temporary character the appendix is included in the preprint version of the paper only [14].

Some results of the tests and improvements of PHOTOS, relevant to τ physics, have already been discussed in [15].

2 Physical problem and developed solution

Although QED bremsstrahlung in particle decays is one of the most elementary effects in quantum mechanics, it is not usually considered explicitly; to simplify, calculations

are performed for inclusive quantities. In fact, it is only the case of a few specific decay channels, where exact fixed-order (e.g. $O(\alpha^2)$) fully differential formulae, with spin amplitudes or matrix elements squared, are available in analytical, semi-analytical or Monte Carlo form. Nonetheless, in the analysis of the experimental data, radiative corrections are usually treated together with the detector effects (e.g. conversion, detector efficiency) to form the "QED-subtracted" data. The control of the uncertainties of such data becomes a weak point: theoretical uncertainties appear on both sides of the "*theory = experiment*" equation [16]. This problem does not seem to be so evident for "discovery" experiments or measurements performed on small statistical samples: usually the effects of radiative corrections do not exceed a few per cent.

Conversely, for high-precision measurements (as those performed nowadays), good control of the radiative corrections becomes vital not only for the assessment of the overall experimental error of the respective cross-sections or branching ratios, but also for the shapes of the distributions.

The effects of radiative corrections gradually became an important topic in the context of such measurements as high-precision measurements of W-boson properties (see, for instance, the combined results of Tevatron runs [4]), or B, D, K meson decays for measurements of CKM-matrix coefficients in B physics [17]. With increasing statistics of available experimental data, QED radiative corrections have become a significant element in the systematic error of the measured quantities.

Strict, systematic calculations performed order-by-order in the perturbation theory are usually not the most efficient way of including the effects of bremsstrahlung. To improve the convergence of the perturbative expansion, the most popular method in QED is exponentiation, a rigorous scheme of reshuffling the dominant terms between orders of expansion. This method is useful for the construction of Monte Carlo algorithms as well [18,19]. In the leading-log approximation, partially inclusive formulae exhibit factorization properties of QED; see e.g. [20]. A matrix element formula for particle decay accompanied by bremsstrahlung photon emission may be factorized to Born-level terms times the bremsstrahlung factor[1].

Similarly, a fully differential formula for Lorentz-invariant phase space for particle decay accompanied by a number of photons may be expressed in a way that exhibits factorization properties. It is used, for example, in the construction of the TAUOLA algorithm for $l\nu_\tau\bar{\nu}_l(\gamma)$ [23]. The important property of this parametrization is the full coverage of the phase space and the exact (i.e. free of approximations) treatment. The price to pay is that the variables describing each added photon are defined in individual rest frames, separated by boosts, making the question of the

choice of gauge fixing a very subtle point of the theoretical bases of the algorithm [24].

As a result of the studies of the second-order matrix element, in particular for $Z \to \mu^+\mu^-\gamma\gamma$ and $gg \to t\bar{t}\gamma\gamma$ (performed already in 1994 [25,26]), the iterative properties of the bremsstrahlung-adding formula have been identified and a universal photon-emission kernel has been isolated and double-photon emission implemented in PHOTOS. However, at that time, the question of precision was left out of the discussion. The main application was an estimate of the background to the Higgs boson searches in the $H \to \gamma\gamma$ channel. Only double hard-photon bremsstrahlung was of interest, and a precision of about 10% on the cross-section was sufficient.

3 Main features of the PHOTOS algorithm

PHOTOS is an "after-burner" algorithm, which adds bremsstrahlung photons to already existing events, filled in by a host generator (which does not take into account the effects of QED radiative corrections) and transmitted by means of a standard HEPEVT event record (only the information about four-vectors of particles taking part in the process and the topology of the process are needed). PHOTOS adds (with a certain probability) final-state QED radiation in "any" decay of particle or resonance, independent of the physics process that was generated. As the result of its execution, bremsstrahlung photons are added in a fraction of the events in the HEPEVT event record, taking into account event topology and momentum conservation.

The single-photon version of the PHOTOS algorithm originates from the MUSTRAAL Monte Carlo [21,22], in its part for the $Z \to \mu^+\mu^-(\gamma)$ process. The original algorithm, although maintaining full $O(\alpha)$ precision and exposing factorization properties, was however dependent on the underlying process[2]. A downgrade was therefore required to make the algorithm process independent: the interference terms were removed from the formula, and later restored in an approximated way for a limited set of processes (decays of neutral particles into two charged particles of the same mass) by introducing a Monte Carlo interference weight.

In the iterative algorithm for (fixed-number) multiple-photon emission in PHOTOS, the probability of photon generation is based (at crude level) on a binomial distribution, i.e. the probability for generating and not generating a photon is calculated in each iteration. Encouraged by the precision of PHOTOS with a photon multiplicity higher than 2 (subsequent terms in the expansion improved the agreement with exact calculations), we decided to replace the binomial distribution with a Poissonian distribution for the number of photons to be generated. In this new Poissonian mode, the algorithm is no longer limited to a fixed maximal number of photons: the actual number of photons is also generated (at this "crude-generation" level). The modification set the algorithm free from the

---

[1] For some cases this factorization property is also present for non-approximated formulae, e.g. for the $O(\alpha)$ ME formula for Z-boson decays as implemented in MUSTRAAL [21,22] at fully differential level. In [1] it was shown, contrary to the previous expectations, that this factorization has a natural geometrical interpretation as well.

[2] It remains implemented in the first published version of KORALZ 3.8 [27], with multiple initial-state bremsstrahlung and single final-state radiation.

negative-probability problem as well. At a crude level, the total probability for single-photon emission in the iterated kernel does not need to be smaller than 1, because it is multiplied by the exponent of an equally large, but negative, number[3]. Because the crude distribution resembles an expansion of an exponent we call this version of multiple-photon algorithm an "exponentiated mode" of PHOTOS. Our approach is also close to the language of exponentiation as known in QED since Yennie–Frautchi–Suura times [28]. The exponentiated mode has proved to be more stable, allowing us to significantly lower the value of the infrared cut-off on the photon energy as well.

A flexible organisation of iteration [29] and phase-space variables in the PHOTOS algorithm not only allows for a full phase space coverage, but also seems to introduce some higher-order effects, as will be discussed later in the paper (Sect. 5.2). This was achieved by careful studies and comparisons with matrix-element calculations [24–26], without need of any kind of phase-space ordering.

Problems with the numerical stability may occur when the four-vectors passed in the event record have insufficient precision. PHOTOS is very sensitive to rounding errors and momentum conservation in the event record, especially when the multiple-photon-emission mode of operation is used. At each iteration of the photon-emission kernel numerical rounding errors are accumulated.

Driven by the needs of B-physics experiments, a new, universal interference weight was implemented, allowing for the calculation of an interference for "any" process (see also Sect. 5.4). Although the formula for this interference weight is given already in (17) of [2], its integration with the PHOTOS code was not trivial until work presented in [30]; it was this modification for W decays, that made the implementation possible for every decay.

From the point of view of the precision of the obtained results, the PHOTOS algorithm may work in three regimes:
(1) as a "crude-level" tool for bremsstrahlung generation in decays of any particle or resonance,
(2) as a precision tool for dedicated decay channels (at present Z and W decays),
(3) as a precision tool incorporating matrix-element calculations (not exploited so far).

At a "crude level", only the leading-log soft-photon parts of the matrix element should be expected to be correctly included in the PHOTOS algorithm[4]. PHOTOS is most often used as a general-purpose tool, thus working at the "crude level" of precision. The precision of the results cannot be guaranteed in this working regime; a typical example of use could, however, be the generation of full bremsstrahlung phase-space coverage for acceptance studies only.

For the particular decay channel, the PHOTOS algorithm could then be upgraded to regime (2) or (3), depending on the form of the necessary compensating weight. At present, the algorithm employs a number of improvements (with the help of the correcting weight) and takes into account such effects as the threshold terms for fermions and the impact of the spin of the emitting particle. Other effects (e.g. the impact of spin of a decaying particle or the influence of spin on interference terms) are not at present taken into account.

The impact of the approximations and missing terms on the precision of PHOTOS, when used in regime (2), that is for W and Z decays, is the main subject of this paper.

4 Test definition

Our approach to the study of precision of the PHOTOS algorithm presented in this paper is based on numerical comparisons of results obtained from PHOTOS with respect to the results produced by other *reference* Monte Carlo generators. The reference generators that we used employ formulae based on the full (i.e. non-approximated) fixed-order matrix-element calculations with or without exponentiation; their precision level is well established, both by theoretical considerations and by comparisons with experimental data. The advantage of such an approach is obvious: it allows us not only to check the theoretical precision of the approximation used, but also verifies that there are no accidental errors in the actual computing code.

This approach is probably more appealing to the practically-oriented user than to the theoretically-oriented one. We leave more profound theoretical studies for the future, to be possibly performed in the context of feasibility studies of the applicability of methods used in PHOTOS to QCD.

We have tested PHOTOS against a limited number of event generators and for a limited number of processes. The choice of processes was dictated not only by physics interests, but also by the availability of Monte Carlo generators with well-controlled and established precision. The following processes were studied.
(1) $Z^0 \to \mu^- \mu^+$: for this process the LEP era generators KORALZ [19,31] and KKMC [18] could be used. Note that these programs agreed well with practically all experimental data of the LEP measurements. The KKMC generator is based on $O(\alpha^2)$ ME calculations with spin-amplitudes technique and exponentiation. It can also be used in $O(\alpha)$ ME exponentiated mode. In the case of KORALZ, generation at first-order matrix element and no exponentiation were available as well.
(2) $W^+ \to \mu^+ \nu_\mu(\gamma)$: for this process the WINHAC [32] generator is available for multiple photon generation in decay. It is based on first-order matrix element and exponentiation. Comparison of PHOTOS with a first-order matrix-element generator without exponentiation can be found in [30]; we will not repeat it here.
(3) $H \to \mu^+ \mu^-(\gamma)$: comparison of PHOTOS with a first-order matrix-element generator without exponentiation

---

[3] This is trivial: if p is the probability in the binomial distribution, it must be smaller than 1; however it does not need to have in a Poissonian distribution given by $P_n = \frac{1}{n!} e^{-p} p^n$.

[4] It can be estimated that the physical uncertainty of the PHOTOS algorithm, with double emission and working on the decay of particle P into a charged particle ch and the neutral system Y_i, is then not smaller than $\frac{\alpha}{\pi}$ or $\left(\frac{\alpha}{\pi} \log \frac{m_P^2}{m_{ch}^2} \right)^3$, whichever is bigger.

can be found in [33]; we will not repeat it here.

(4) For leptonic τ decays, complete QED first-order generation with the TAUOLA [23] generator was available for tests; TAUOLA was widely used and compared successfully with LEP and CLEO data [34, 35].

The event generators and physical initializations mentioned above will be referred to as "reference generators". They were used to produce reference results used in comparisons with PHOTOS.

The testbed constructed from the event generators discussed above had one very important feature: it allowed a test of PHOTOS against several algorithms that differ in physical content and precision. Tests started from an exact $O(\alpha)$ matrix element for single-photon emission (non-exponentiated KORALZ and TAUOLA compared with a single-photon version of PHOTOS), and went on to multiple-photon generators (exponentiated versions of KKMC, KORALZ and WINHAC) compared with triple-, quartic- and exponentiated multiple-photon modes of PHOTOS.

To operate, PHOTOS needs events produced by a "host" generator as an input. We exploited the possibility of deactivating the bremsstrahlung generation in reference generators, to turn them into QED Born-level "host" generators.

Let us now define the method for automated tests that were used to obtain the results presented later in this paper. To facilitate the systematic comparisons, we adopted a specially designed tool: MC-TESTER, described in detail in [36]. The principle of an underlying test is to analyze the series of events produced by two distinct Monte Carlo event generators (or a sequence of several generators combined together) and to extract characteristic distributions in an automatic way. In practice, we search for distinct decay channels of the particle of interest and store histograms with distributions of all invariant masses that can be formed from the four-momenta of its decay products.

For a selected decay process, in cases discussed here, Z, W and τ decays, the distributions are extracted from the event record in an automated way (thereby limiting the effort for setting up the appropriate analysis code, and also the risk of accidental errors) and stored in the output files. Two output files (from distinct runs of event generators instrumented with MC-TESTER) are then analyzed, and the results are presented in a form visualized as a "booklet" of plots and tables. The user is given general information concerning two compared runs of Monte Carlo generators, a list of the decay channels with their branching fractions, and the maximum values (for each decay channel) of the shape difference parameter (SDP)[5]. For each decay channel

the plots of histogrammed values are then included: each plot presents the two distributions from two distinct runs, and the curve being a ratio of the normalized distributions; the value of the SDP is also printed for each plot.

The testing approach implemented in MC-TESTER was already very useful in the case of validation of the TAUOLA package; however, for the purpose discussed here it required further adaptation. The problem was in the consistent treatment of the arbitrary number of final-state QED bremsstrahlung photons that might be present in the event, the ambiguity caused by infrared singularities of QED, which is handled differently by the various Monte Carlo programs.

Our aim was to develop a technique where comparisons would make physical sense, would be automatic and independent of the way infrared singularities are regularized in particular generators. For our analysis, we defined zero-, one-, and two-photon topologies in the following way: we called the event "zero photon" if there was no photon of energy (in a decaying particle rest-frame) larger than the parameter E_{test}. The "one-photon" event had to have one (and only one) photon of energy larger than E_{test}. If there were more than one such photon, we called it a "two-photon" event. If there were more than two photons of energy larger than E_{test}, we considered only the two most energetic ones, and treated the remaining ones as if they had not passed the E_{test} threshold. For all the photons that did not pass the E_{test} threshold we performed an operation inspired by leading-log logic: we added their four-momenta to the momenta of outgoing fermions of smaller angular separation.

We defined two variants for this test definition: *test1* and *test2*. The *test2* was exactly as explained above. In *test1*, only one photon (the most energetic one) could be accepted[6]. The free parameter of the test, E_{test}, was adjusted for each process so that the results had physical sense.

Because of the space limitation we cannot present complete "booklets" with results of comparisons; for the purpose of this paper we decided to extract the most vital information: the branching ratios for events with 0, 1 and 2 photons (0 and 1 if *test1* was used) and the maximum value of SDP throughout all the plots in a channel. Complete results with summary tables and all analysis booklets are available on the web [37]. The tests were based on high-statistics runs (10^8 non-weighted events) for all generators.

Finally, let us stress that an essential preliminary step for the tests presented here was to assure the numerical stability of PHOTOS. As a consequence, we could determine that PHOTOS may be used for processes at very high energies (i.e. at the scale of LHC energies and even at astrophysical ones). The infrared cut on the photon energy may be lowered to 10^{-7} from the 10^{-2} value that had to be used before, when the option for the exponentiated mode was not available.

---

[5] The shape difference parameter defined in [36] quantifies the difference in shape of the histograms coming from two compared runs. The histograms contain distributions of all possible invariant masses, which can be constructed from the momenta of the decay products of the particle under study; hence there is a set of histograms for every decay channel. The SDP value is calculated for each histogrammed mass: it quantifies the exclusive surface between the (normalized to unity) corresponding histograms obtained from the two runs. The effects of statis-

---

tical fluctuations are appropriately subtracted. The maximum of SDP over all distributions for a given decay channel is taken.

[6] If needed, this scheme could be generalized, for instance, to define *test3*, where up to three photons of energies above E_{test} could be accepted, leading to a fourth distinct decay channel.

5 Numerical results

The results presented here cover two issues: the precision of the predictions obtained for the single-photon-emission kernel and the convergence of the iterative solution. At first, in Sect. 5.1, we will discuss the comparisons of a single-photon-emission kernel implemented in PHOTOS with other genuine first-order generators. In Sect. 5.2, we will discuss tests for multiple-photon generation. Finally, in Sect. 5.3, we will discuss the applicability of PHOTOS at very high energies.

As mentioned before, we aim at comparing, in total, *six* versions of distinct Monte Carlo programs with five distinct modes of executing PHOTOS. Let us specify them here (including acronyms that will be used throughout the text).
(1) KORALZ O(1): KORALZ [31] with $O(\alpha)$ ME for $Z^0 \rightarrow \mu^+\mu^-(\gamma)$, no exponentiation, single-photon emission;
(2) KORALZ: KORALZ [31] with $O(\alpha^2)$ ME for $Z^0 \rightarrow \mu^+\mu^-(\gamma)$ and exponentiation (multiple-photon emission);
(3) KKMC: KKMC [18] with $O(\alpha^2)$ ME for $Z^0 \rightarrow \mu^+\mu^-(\gamma)$ and exponentiation at spin-amplitudes level;
(4) KKMC $O(1)_{\text{EXP}}$: KKMC [18] with $O(\alpha)$ ME for $Z^0 \rightarrow \mu^+\mu^-(\gamma)$ and exponentiation;
(5) TAUOLA: TAUOLA [23] with $O(\alpha)$ ME for $\tau \rightarrow l\bar{\nu}_l\nu_\tau(\gamma)$ (single-photon emission);
(6) WINHAC EXP: WINHAC [32] with full $O(\alpha)$ ME for $W \rightarrow l\bar{\nu}_l(\gamma)$ and exponentiation;
(7) PHOTOS O(1): PHOTOS, no iteration;
(8) PHOTOS O(2): PHOTOS algorithm iteration up to two times;
(9) PHOTOS O(3): PHOTOS algorithm iteration up to three times;
(10) PHOTOS O(4): PHOTOS algorithm iteration up to four times;
(11) PHOTOS EXP: PHOTOS algorithm with exponentiation, multiple-photon generation.

Before we proceed with a presentation of the results, let us, however, briefly describe the approach taken for this presentation and their numerical quantification.
(1) As described in Sect. 4, we quantify the difference between results produced by two generators by calculating branching ratios for events with 0, 1 or 2 photons with energy above the E_{test} threshold, and the maximum values of the SDP parameter of all combinations of invariant masses in the specific channel (with 0, 1 or 2 photons) for a given comparison.
(2) In the discussion of the results we will also often use a single value of the "overall difference", being either the maximum of differences in branching ratios or the maximum of products of SDP and corresponding branching ratios[7]. We then take the larger of the two and express it in per cents.

Later in this section we present only the simplified summary tables and plots where the differences in distributions (quantified by the SDP parameter) are most significant. In

the summary tables the first line (appearing in bold font) refers to the results produced by the reference generator, the others refer to results of runs of generators being tested.

5.1 Single-photon emission kernel

In this subsection we focus on the quality of the single-photon emission kernel in the PHOTOS algorithm. We perform a systematic comparison of PHOTOS with generators that implement $O(\alpha)$ matrix element for Z, W and τ decays.

The purpose of these tests was to assess the impact of the simplifications of the photon-emission kernel implemented in PHOTOS on the precision of its predictions (in the PHOTOS kernel the non-leading $O(\alpha)$ terms are omitted).

At first, let us present the comparisons made in the $Z \rightarrow \mu\mu(\gamma)$ channel. In fact, the original PHOTOS algorithm was created by gradual simplification of the exact ME formula for this process, so the universal emission kernel could have been identified. Therefore this process remains a benchmark for PHOTOS single-emission algorithm, its precision and design. The approximations are well understood and may in fact be restored for this particular case.

We compare PHOTOS with KORALZ Monte Carlo in single-photon emission mode. This test, which was already performed a long time ago (when PHOTOS was being developed), has been reproduced now, and confirmed that no accidental error has occurred since then. The results of this comparison are presented in Fig. 1.

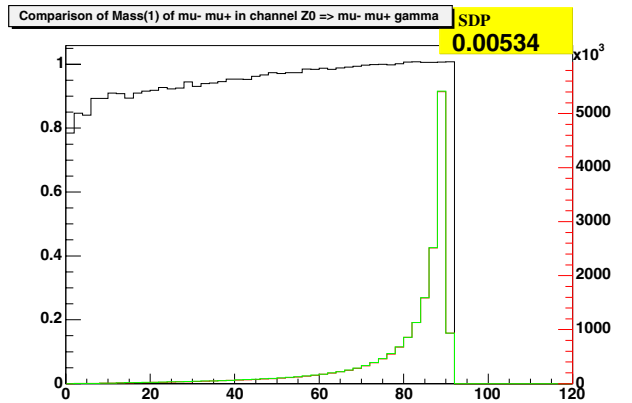| GENERATOR	Branching ratio		Max SDP	
n photons $\rightarrow$	0	1	0	1
KORALZ O(1)	**0.82514**	**0.17486**		
PHOTOS O(1)	0.82362	0.17638	0	0.0053

Fig. 1. Predictions of KORALZ (with $O(\alpha)$ matrix element and single-photon emission) are compared with predictions of PHOTOS (running in single-photon option) for the $Z^0 \rightarrow \mu^+\mu^-(\gamma)$ channel, $E_{\text{test}} = 1.0\,\text{GeV}$. The plot presents the distribution of the invariant mass of a $\mu^-\mu^+$ pair coming from KORALZ (in red, or darker-grey) and PHOTOS (in green, or lighter-grey); the black line is the ratio of the two normalized distributions. The red and green lines are hard to separate – they practically overlap

---

[7] For instance, in case of the table in Fig. 1 the difference in branching ratios is $0.82514 - 0.82362 = 0.00152$, the product $\text{SDP} \times \text{BR} = 0.0053 * 0.176 = 0.00093$, so that the first value is taken as the overall difference for that test: 0.152%.

One may notice that the difference in branching ratios for channel with and without photon are at the per mil level. The differences in distributions (the maximum value of SDP multiplied by branching ratios) indicate agreement better than per mil: we have quantified the overall difference as 0.15%.

The dominant contribution to the difference originates from a very sparsely populated area of the phase space, where the invariant mass of the lepton system is small, and very hard photons were emitted. The discrepancy between the distributions does not exceed 20%, even in this corner of the phase space, though. It is visible in the slope of the black curve denoting the ratio of the two distributions. In this region of the phase space the approximations (with respect to $O(\alpha)$) used in PHOTOS are the largest. The differences are too small to justify the implementation of a channel-dependent correction weight. For the case of W-boson decays, we refer the reader to [30], where the comparison of PHOTOS and a $O(\alpha)$ ME generator SANC [38][8] for the $W \to \mu\bar{\nu}_\mu(\gamma)$ process is given. This paper provides also the theoretical background for the W interference weight implemented in 2003 in PHOTOS 2.07. The presented tests indicate a very good agreement between PHOTOS and SANC: up to a level of 1% (statistical error) in the majority of the areas of the phase space, within 5% for parts of distributions where collinear-induced logarithms are absent and 10% in the regions where only non-leading corrections contribute to the matrix element. The paper [33] presents the comparison of various distributions from PHOTOS and SANC [38] generators for Higgs boson decays: an agreement at the level of 1% (statistical error) was found all over the phase space.

We consider the results of these tests, published in relatively recent papers [30, 33], as being relevant and complementary to the tests presented here. Therefore we do not repeat the comparison of WINHAC generator [32] and PHOTOS in single-photon emission mode.

We have however exploited the opportunity of having another comparison with full $O(\alpha)$ matrix element generator, that is TAUOLA [23] for leptonic τ decays. The results of the comparison in the $\tau^- \to \mu^- \bar{\nu}_\mu \nu_\tau(\gamma)$ decay channel are presented in Fig. 2. The overall difference was quantified as 0.11%. The agreement between the PHOTOS and TAUOLA results is excellent. In the $\tau^- \to e^- \bar{\nu}_e \nu_\tau(\gamma)$ channel, the agreement is equally good.

5.2 Iterating emission kernels

In this subsection we cover the comparisons of PHOTOS with other generators for multiple-photon generation. In multiple-photon mode, the PHOTOS algorithm iterates the single-photon-emission kernel, of which the precision was established in the previous subsection. The main questions to be answered by the group of tests presented here were the

---

[8] SANC calculates complete one-loop amplitudes for the decays of on-shell vector bosons: W, Z or the standard model Higgs boson; an exact, single, real-photon emission matrix element is obtained that way.

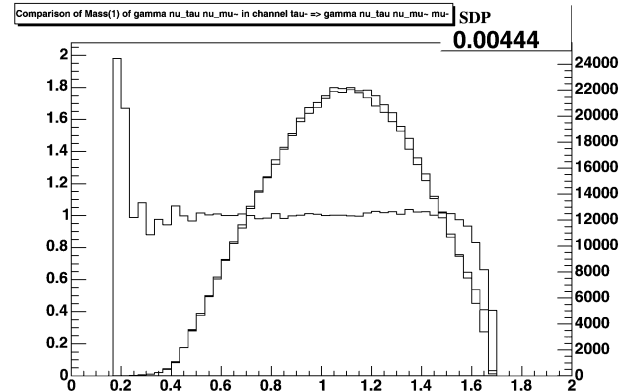| GENERATOR	Branching ratio		Max SDP	
n photons $\to$	0	1	0	1
TAUOLA	**0.98916**	**0.01084**		
PHOTOS O(1)	0.98927	0.01073	0	0.0044

Fig. 2. Predictions for exact $O(\alpha)$ in TAUOLA are compared with single-photon emission of PHOTOS in the $\tau^- \to \mu^- \bar{\nu}_\mu \nu_\tau(\gamma)$ channel, $E_{\text{test}} = 0.05\,\text{GeV}$. The plot presents the distribution of the invariant mass of the $\bar{\nu}_\mu \nu_\tau \gamma$ system coming from TAUOLA (in red, or darker-grey) and PHOTOS (in green, or lighter-grey); the black curve is the ratio of the two normalized distributions

ones concerning the convergence of the PHOTOS iterative algorithm for photon emission to solutions implemented in other generators.

The KKMC Monte Carlo program [18] played an important role in multiple-photon comparisons: it is the only available Monte Carlo routine that implements a complete $O(\alpha^2)$ matrix element for two hard-photon emission in the $Z \to \mu^+ \mu^- n(\gamma)$ channel. Because of its superior quality with respect to KORALZ [31] (which implements $O(\alpha^2)$ ME with more approximations) it was used as the reference generator throughout all tests in this channel. Before continuing with tests of PHOTOS let us first compare the KORALZ and KKMC Monte Carlo programs to assess the impact of the presence of second-order terms in the calculations. The results of comparisons performed using *test1* are presented in Fig. 3. The overall difference is below a per mil level; however, with samples of 10^8 events the contribution from those $O(\alpha^2)$ terms that are missing in KORALZ is already visible. As will be shown later, the differences are in fact at the level of (and are comparable in shapes to) the differences observed between KORALZ and PHOTOS.

We start the tests of PHOTOS from comparisons for the benchmark decay $Z \to \mu^+ \mu^- n(\gamma)$. The complete summary of results is presented in Table 1 (as usual, complete results, with MC-TESTER booklets are available from the web page [37]).

We tested PHOTOS running with various options for photon multiplicity: fixed (two to four) order and the exponentiated versions against the reference KKMC generator.

We observed that adding subsequent iterations of the photon-emission kernel improves the agreement between

Table 1. Summary of multiple-photon comparisons in $Z^0 \to \mu^+\mu^- n(\gamma)$ channel (Z^0 at resonance peak, CMS rest-frame); $E_{\text{test}} = 1.0\,\text{GeV}$. KKMC was used as a reference generator. For KKMC–KORALZ comparison the overall difference is 0.066%, for KKMC–PHOTOS EXP it is 0.081%, for KKMC–KKMC $O(1)_{\text{EXP}}$ it is 0.137% (all differences are for *test1*)

GENERATOR	Branching ratio					Max SDP				
	test1		test2			test1		test2		
n photons $\to$	0	1	0	1	2	0	1	0	1	2
KKMC	**0.83918**	**0.16082**	**0.83918**	**0.14816**	**0.01266**					
KORAL Z	0.83984	0.16016	0.83984	0.14771	0.01244	0	0.0021	0	0.0012	0.0012
PHOTOS O(2)	0.83925	0.16075	0.83925	0.14630	0.01445	0	0.0067	0	0.0035	0.0122
PHOTOS O(3)	0.83832	0.16168	0.83832	0.14889	0.01280	0	0.0038	0	0.0025	0.0080
PHOTOS O(4)	0.83836	0.16164	0.83836	0.14871	0.01293	0	0.0040	0	0.0027	0.0058
PHOTOS EXP	0.83837	0.16163	0.83837	0.14868	0.01295	0	0.0041	0	0.0023	0.0092
KKMC $O(1)_{\text{EXP}}$			0.83781	0.14881	0.01338			0	0.0099	0.0467

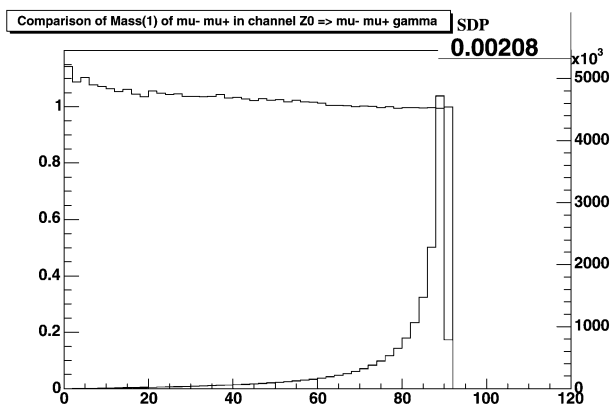| GENERATOR	Branching ratio		Max SDP	
n photons $\to$	0	1	0	1
KKMC	**0.83918**	**0.16082**		
KORALZ	0.83984	0.16016	0	0.0021

Fig. 3. Comparison of predictions from KKMC ($O(\alpha^2)$ ME with exponentiation at the level of spin amplitudes) and KORALZ ($O(\alpha^2)$ ME with exponentiation) in the $Z^0 \to \mu^+\mu^-(\gamma)$ channel, $E_{\text{test}} = 1.0\,\text{GeV}$, *test1* used for analysis. The plot presents the distribution of the invariant mass of a $\mu^+\mu^-$ pair coming from KKMC (in red, or darker-grey) and KORALZ (in green, or lighter-grey); the black line is the ratio of the two normalized distributions. The effects due to different types of exponentiation are small, albeit noticeable, and constitute 0.066% overall difference

PHOTOS and KKMC. The difference in the results between quartic-iteration and exponentiated version of PHOTOS are negligible; however, the exponentiated version is technically superior, because it may work with a much lower value of the infrared cut-off parameter (see the appendix of [14] for details).

It is striking that the agreement between the exponentiated versions of PHOTOS and KKMC is best if the full $O(\alpha^2)$ exponentiated matrix element is used in KKMC; if

KORALZ with exponentiated $O(\alpha)$ is used[9] or the matrix element in KKMC is downgraded to exponentiated $O(\alpha)$ only (see the last row in the table), the agreement is not as perfect, but it is still good enough for any application we can imagine at present.

The dominant differences are visible in the branching fractions for channels with distinct numbers of photons with energies above E_{test}. The pattern of differences may indicate that leading terms summed by an iterated PHOTOS kernel give a better precision than any first-order exponentiated ME generator for this process.

To investigate this hypothesis further, we have turned our attention to acoplanarity distributions obtained from PHOTOS and KKMC. One of the effects brought about by NNLO terms of $O(\alpha^2)$ ME is the asymmetry in the acoplanarity distributions. To define acoplanarity, the two planes are spanned on momenta vectors of μ^- and the two hardest photons. In Fig. 4a we show the acoplanarity distributions from the KKMC generator with $O(\alpha^2)$ and $O(\alpha)$ exponentiated matrix-element modes[10]. As expected, the distribution is flat for the $O(\alpha)$ exponentiated mode and asymmetry appears for the $O(\alpha^2)$ exponentiated mode only.

In Fig. 4b we present the acoplanarity distributions from the exponentiated $O(\alpha^2)$ ME mode of KKMC and exponentiated version of PHOTOS. Surprisingly, PHOTOS seems to reproduce the bulk of this NNLO effect! This rather subtle effect requires investigation. PHOTOS does not use any kind of phase-space ordering, but, at the time when the second photon is generated, the momentum of the previous one is changed and so the correlations between the directions of two photons appear. We shall not elaborate further on this effect here; however, we believe that further enhancements of the precision of the PHOTOS algorithm in this respect may be possible, for instance by introducing an asymmetry in the generation of a photon polar angle (a uniform distribution is currently used in the emission kernels).

---

[9] These results are not included in this paper.

[10] In order to make the effect visible, we used the following cuts: only the events with both photons in the same hemisphere as μ^- and having $p_{\text{t}} > 1.5\,\text{GeV}$ were recorded in the histogram.

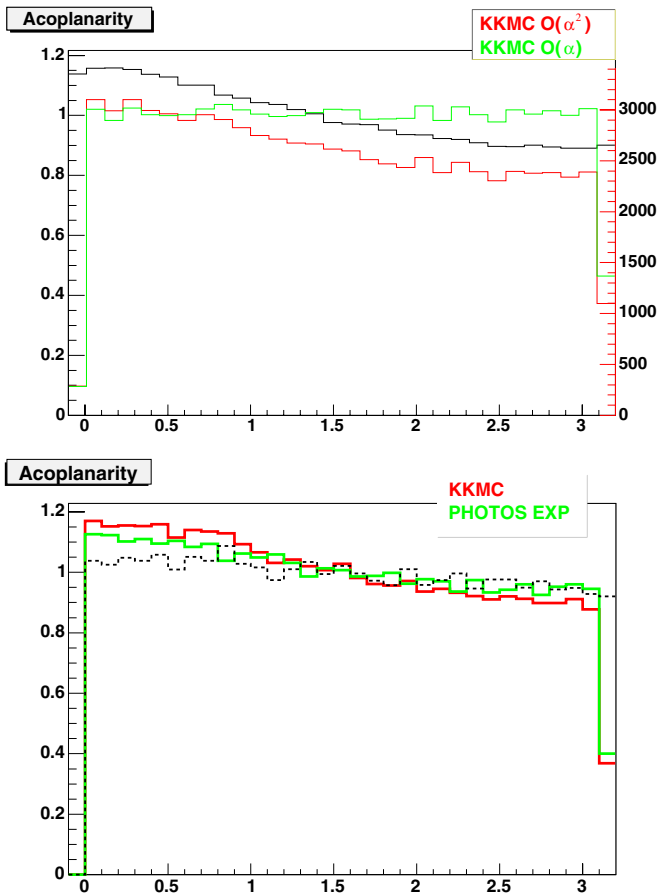**Fig. 4.** Acoplanarity distributions in the $Z^0 \to \mu^-\mu^+\gamma\gamma$ channel. The ratios of the distributions are plotted in black. For more details see Sect. 5.2. **a** Comparison of KKMC in exponentiated $O(\alpha^2)$ mode (in red, or darker-grey) and exponentiated $O(\alpha)$ mode (in green, or lighter grey). **b** Comparison of KKMC in exponentiated $O(\alpha^2)$ mode (in red, or darker-grey) and the exponentiated PHOTOS algorithm (in green, or lighter grey)

Let us now present the results of the comparisons of the exponentiated mode of PHOTOS and full $O(\alpha)$ exponentiated ME predictions of WINHAC for the $W \to l\bar{\nu}_l(\gamma)$ channels. Both programs were running in exponentiated mode. The complete summary of results is presented in Table 2.

The details of one of these comparisons are presented in Fig. 5. The overall agreement is better than per mil. The maximum value of SDP in configurations with two hard photons are larger for some tests (reaching the level of 0.0255 in the last row of the table); however, this is a channel with rather small branching fraction.

Finally, let us turn to $\tau^- \to \mu^-\nu_\tau\bar{\nu}_\mu(\gamma)$ decay. The comparison of predictions from the exponentiated version of PHOTOS and full $O(\alpha)$ ME of TAUOLA are presented in Fig. 6. The overall agreement is better than 0.02%.

It is interesting to compare the results presented in Fig. 6 with the results in Fig. 2, where exact TAUOLA is compared with the single-photon mode of PHOTOS. One can notice that the difference between the single-photon-emission mode in PHOTOS and TAUOLA is similar to the difference between the exponentiated mode of PHOTOS

GENERATOR	Branching ratio		Max SDP	
n photons $\to$	0	1	0	1
WINHAC (EXP)	**0.92771**	**0.07229**		
PHOTOS (EXP)	0.92748	0.07252	0	0.0029

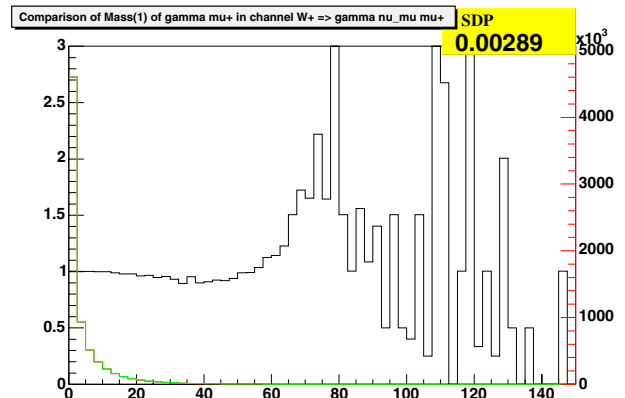**Fig. 5.** Multiple-photon comparison of WINHAC and PHOTOS (both running in the exponentiated mode) in the $W^+ \to \mu^+\nu_\mu n(\gamma)$ channel, $E_{\text{test}} = 1.0$ GeV, analyzed using *test1*. The plot (of largest SDP) presents the distribution of the invariant mass of the $\mu^+\gamma$ pair coming from WINHAC (in red, or darker-grey) and PHOTOS (in green, or lighter-grey); the red and green lines practically overlap. The black line is the ratio of the two normalized distributions

GENERATOR	Branching ratio		Max SDP	
n photons $\to$	0	1	0	1
TAUOLA	**0.98916**	**0.01084**		
PHOTOS EXP	0.98935	0.01065	0	0.0047

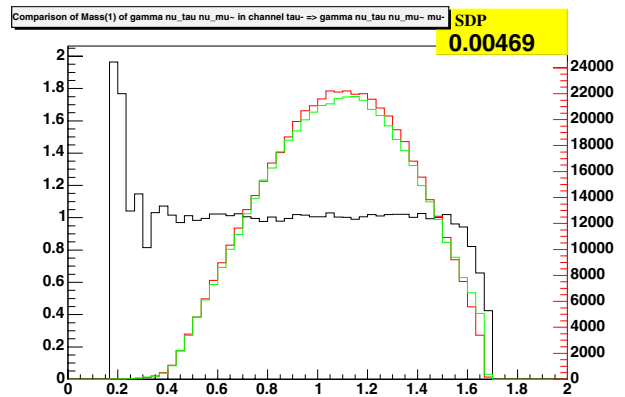**Fig. 6.** Comparison of full $O(\alpha)$ in TAUOLA and exponentiated version of PHOTOS for $\tau^- \to \mu^-\nu_\tau\bar{\nu}_\mu(\gamma)$ channel, $E_{\text{test}} = 0.05$ GeV, *test1* is used. The plot below presents the distribution of invariant mass of $\nu_\tau\bar{\nu}_\mu\gamma$ from TAUOLA (in red, or darker-grey) and PHOTOS (in green, or lighter-grey); the black curve is the ratio of the two normalized distributions

and TAUOLA. This indicates that the dominant source of differences is due to non-leading $O(\alpha)$ terms that are missing in PHOTOS (and present in full $O(\alpha)$ ME of TAUOLA). Predictions of the single-photon mode of TAUOLA are more precise than PHOTOS predictions, even with exponentiation. Nevertheless, it must be realized that as

Table 2. Summary of comparisons of the exponentiated algorithm of PHOTOS and WINHAC $O(\alpha)$ exponentiated for leptonic W decays. For more details, see the text

GENERATOR	Branching ratio					Max SDP				
	test1		test2			test1		test2		
n photons →	0	1	0	1	2	0	1	0	1	2
$W^+ \to \mu^+\nu_\mu(\gamma)$ at W mass, $E_{\text{test}} = 1.0\,\text{GeV}$										
WINHAC EXP	**0.92771**	**0.07229**	**0.92771**	**0.07007**	**0.00222**					
PHOTOS EXP	0.92748	0.07252	0.92748	0.07016	0.00236	0	0.0029	0	0.0025	0.0023
$W^+ \to \mu^+\nu_\mu(\gamma)$ at W mass, $E_{\text{test}} = 5.0\,\text{GeV}$										
WINHAC EXP	**0.96491**	**0.03509**	**0.96491**	**0.03473**	**0.00036**					
PHOTOS EXP	0.96470	0.03530	0.96470	0.04488	0.00042	0	0.0060	0	0.006	.047
$W^+ \to e^+\nu_e(\gamma)$ at W mass, $E_{\text{test}} = 1.0\,\text{GeV}$										
WINHAC EXP	**0.86196**	**0.13804**	**0.86196**	**0.12943**	**0.00862**					
PHOTOS EXP	0.86205	0.13795	0.86205	0.12909	0.00886	0	0.0022	0	0.0019	0.0094
$W^+ \to e^+\nu_e(\gamma)$ at W mass, $E_{\text{test}} = 5.0\,\text{GeV}$										
WINHAC EXP	**0.93083**	**0.06917**	**0.93083**	**0.06763**	**0.00153**					
PHOTOS EXP	0.93087	0.06913	0.93087	0.06747	0.00166	0	0.0046	0	0.0041	.0255

TAUOLA does not implement exponentiation, it is limited to the generation of (at most) single hard-photon emission. For cases where the topologies of configurations with two or more photons are important, the exponentiated algorithm implemented by PHOTOS will be more appropriate.

5.3 Tests of PHOTOS at very high energies

Because of numerical instabilities, the use of PHOTOS at LHC energies of 14 TeV was technically limited before, by a restriction on the minimal $\frac{E_\gamma^{\min}}{M}$ ratio (M being the mass of the decaying particle, $E_\gamma^{\min}$ the minimal energy of the generated photons). The phase space for generation had to be significantly reduced and photons of even moderate energies could not be generated.

We verified that the exponentiated version of the algorithm, armed with the new kinematics-correction routine implemented in PHOTOS 2.13, allows it to be used to generate bremsstrahlung in decays of very energetic particles at the energy scales that indeed require a very low cut on the minimal photon energy.

We performed studies using KKMC as a "host" generator for PHOTOS to produce leptonic Z decays where the mass of the produced Z/γ intermediate state was of order 2 TeV. The value of the infrared cut-off parameter $\frac{E_\gamma^{\min}}{M}$ was lowered down to the value of $\sim 10^{-7}$, which allowed the generation of relatively soft photons, and high-statistics runs were completed without encountering numerical stability problems. Again, we have found excellent agreement between the exponentiated version of PHOTOS and the exponentiated $O(\alpha^2)$ KKMC. As usual, complete numerical results can be found on the web page [37].

5.4 Recent developments: semileptonic K decays and universal interference weight

Recently our attention was drawn to the use of PHOTOS in an estimation of the effects of QED radiative corrections in high-precision measurements of K, B and D meson decays. The systematic error of the results given by PHOTOS is important for measurements of the elements of the Cabibbo–Kobayashi–Maskawa matrix of quark mixing, because QED corrections affect the acceptance. The insufficient precision of PHOTOS observed in [39] was no surprise: for the case of semileptonic K decays, PHOTOS was prepared for use in the "crude" mode only, suitable for a full phase space coverage of bremsstrahlung for detector studies, but not for shape estimations. The most important missing terms in the calculations performed by PHOTOS in this case were those from QED interference.

Thanks to the technical development performed in PHOTOS, and partially described already in this paper, it was rather straightforward to implement the universal interference weight for any decay channel, as expressed by formula (17) of [2]:

$$W_{\text{multi}} = \frac{\sum_\varepsilon \left| Q_1 \frac{q_1 \cdot \varepsilon}{q_1 \cdot k} + Q_2 \frac{q_2 \cdot \varepsilon}{q_2 \cdot k} + \dots \right|^2}{\sum_\varepsilon Q_1^2 \left| \frac{q_1 \cdot \varepsilon}{q_1 \cdot k} \right|^2 + Q_2^2 \left| \frac{q_2 \cdot \varepsilon}{q_2 \cdot k} \right|^2 + \dots}, \quad (1)$$

where $Q_1, Q_2, \dots$ denote the charges of the decay products, $q_1, q_2, \dots$ denote the momenta of the decay products, k denotes the energy of photon, and a summation is performed over the photon polarization states denoted by ε.

Earlier, the interference weight in PHOTOS was calculated from internal angular variables and not from four-vectors; therefore such a universal implementation was not trivial. The impact of the new interference weight on the photon angle distributions in $K \to \mu\nu\pi(\gamma)$ process is presented in Fig. 7. It seems that the majority of discrepancies

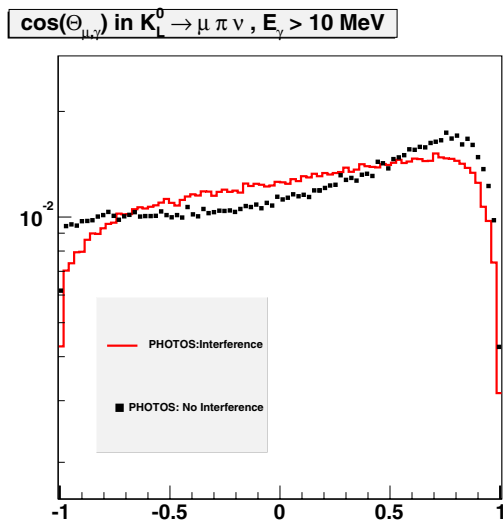**Fig. 7.** Impact of the universal interference weight in PHOTOS on predictions for the angular distribution in $K \to \mu\pi\nu(\gamma)$ events. The distribution of the cosine of the angle between the charged lepton and the photon generated by the older version of PHOTOS, without the interference weight (plotted as black dots), and PHOTOS 2.13 with universal interference weight (plotted as red line). This figure should be compared with Fig. 8b from [39]. The majority of discrepancies between PHOTOS and $O(\alpha)$ generator KLOR seems to be removed by using the universal interference weight

between PHOTOS and the first-order ME generator KLOR have been removed in this way[11]. The complete study will however be documented elsewhere [40].

6 Summary and outlook

We have presented numerical results from a recently upgraded version of the PHOTOS Monte Carlo algorithm for radiative corrections in decays of resonances. In the case of W and Z decays, we found the precision of the simulations in complete multiple-photon final states at the level of (or better than) 0.1%. This conclusion originates from numerous comparisons with precision Monte Carlo programs: KORALZ, KKMC and WINHAC for simulation of radiative corrections in Z and W decays. The reliability of those programs – from the theoretical and technical sides – was well established by numerous applications at LEP time, documented in a multitude of publications on comparisons with the experimental data (in the case of Z decay), as well as other programs and calculations.

The results we presented prove numerically that PHOTOS may be used with confidence to calculate bremsstrahlung in Z and W leptonic decays with a very high precision. In the case of Higgs boson decays and leptonic decays of τs, this precision tag is valid as well, even if the proof is not as solid, since it relies on the test at first order only.

---

[11] For the complete comparison, see Fig. 8 of [39] and our comparison web page [37].

This conclusion cannot be extended to other decay channels, without further work involving a study of process-dependent matrix elements. Nonetheless, the precision in the general case is also better now.

Finally, let us stress that the mathematical side of the multiple-photon algorithm presented here is missing a rigorous proof. Present-day applications do not justify such an effort. Wherever it was possible, we have verified PHOTOS' correctness and found that the performance was excellent. In other cases we were limited by the availability of exact matrix elements for single-photon emission.

A more thorough explanation of the mathematical side of the algorithm may, however, be interesting in the future, especially having in mind applications in QCD. Note that algorithms of PHOTOS do not rely on the conformal symmetry of soft-photon factors and the phase space of massless particles, which is crucial in the construction of exclusive-exponentiation algorithms as used by KKMC, WINHAC or KORALZ.

From its origin, the algorithm of PHOTOS was developed as FORTRAN77 code, even though a C++ implementation was already completed [41] several years ago. Since there was no standard for a C++ event record at that time, it was not published. Recently, the experimental communities expressed interest in using PHOTOS with the HepMC event record [42]. This certainly is a valid option for future development.

References

1. E. Barberio, B. van Eijk, Z. Was, Comput. Phys. Commun. **66**, 115 (1991)
2. E. Barberio, Z. Was, Comput. Phys. Commun. **79**, 291 (1994)
3. M.A. Dobbs et al., hep-ph/0403045
4. CDF Collaboration, V.M. Abazov et al., Phys. Rev. D **70**, 092008 (2004), hep-ex/0311039
5. OPAL Collaboration, G. Abbiendi et al., Phys. Lett. B **580**, 17 (2004), hep-ex/0309013
6. DELPHI Collaboration, J. Abdallah et al., Eur. Phys. J. C **31**, 139 (2003), hep-ex/0311004
7. NA48 Collaboration, A. Lai et al., Phys. Lett. B **602**, 41 (2004), hep-ex/0410059
8. KTeV Collaboration, T. Alexopoulos et al., Phys. Rev. D **71**, 012001 (2005), hep-ex/0410070
9. Belle Collaboration, A. Limosani et al., hep-ex/0504046
10. BABAR Collaboration, B. Aubert et al., Phys. Rev. D **69**, 111103 (2004), hep-ex/0403031
11. FOCUS Collaboration, J.M. Link et al., hep-ex/0412034
12. P. Golonka, Z. Was, in preparation

13. P. Golonka, in preparation; PhD thesis, Institute of Nuclear Physics, Krakow, 2005/2006, written under the supervision of Z. Was; a preliminary version will be available at http://cern.ch/Piotr.Golonka/MC/PhD
14. P. Golonka, Z. Was, hep-ph/0506026
15. Z. Was, P. Golonka, hep-ph/0411377
16. Z. Was, written on the basis of lectures given at the 1993 European School of High Energy Physics, Zakopane, Poland, 12–25 September 1993, CERN-TH-7154-94
17. Radiative corrections in B, D and K meson decays Workshop and CKM05 Conference, La Jolla, March 2005
18. S. Jadach, Z. Wąs, B.F.L. Ward, Comput. Phys. Commun. **130**, 260 (2000), up to date source available from http://home.cern.ch/jadach/
19. S. Jadach, B.F.L. Ward, Z. Wąs, Comput. Phys. Commun. **79**, 503 (1994)
20. P.H. Eberhard et al., to appear in the Proceedings of the Workshop on Z Physics at LEP, edited by G. Altarelli, R. Kleiss, V. Verzegnassi (CERN-89-08 v.1-3) held in Geneva, Switzerland, February 20–21 and May 8–9, 1989; published in LEP Physics Wrkshp.1989:v.1:235-266
21. F.A. Berends, R. Kleiss, S. Jadach, Nucl. Phys. B **202**, 63 (1982)
22. F.A. Berends, R. Kleiss, S. Jadach, Comput. Phys. Commun. **29**, 185 (1983)
23. M. Jezabek, Z. Was, S. Jadach, J.H. Kuhn, Comput. Phys. Commun. **70**, 69 (1992)
24. Z. Was, Eur. Phys. J. C, DOI: 10.1140/epjc/s2005-02381-y
25. E. Richter-Was, Z. Phys. C **64**, 227 (1994)
26. E. Richter-Was, Z. Phys. C **61**, 323 (1994)
27. S. Jadach, B.F.L. Ward, Z. Was, Comput. Phys. Commun. **66**, 276 (1991)
28. D.R. Yennie, S. Frautschi, H. Suura, Ann. Phys. (NY) **13**, 379 (1961)
29. P. Golonka, Z. Was, hep-ph/0508015
30. G. Nanava, Z. Was, Acta Phys. Polon. B **34**, 4561 (2003), hep-ph/0303260
31. S. Jadach, B.F.L. Ward, Z. Was, hep-ph/9905205, Comp. Phys. Commun. in print
32. W. Placzek, S. Jadach, Eur. Phys. J. C **29**, 325 (2003), hep-ph/0302065
33. A. Andonov, S. Jadach, G. Nanava, Z. Was, Acta Phys. Polon. B **34**, 2665 (2003), hep-ph/0212209
34. ALEPH Collaboration, M. Davier, C.-z. Yuan, eConf C0209101 (2002) TU06, hep-ex/0211057
35. CLEO Collaboration, S. Anderson et al., Phys. Rev. D **61**, 112002 (2000), hep-ex/9910046
36. P. Golonka, T. Pierzchala, Z. Was, Comput. Phys. Commun. **157**, 39 (2004), hep-ph/0210252
37. P. Golonka, Z. Was, http://cern.ch/Piotr.Golonka/MC/PHOTOS-MCTESTER
38. A. Andonov et al., hep-ph/0209297
39. T.C. Andre, hep-ph/0406006
40. P. Golonka, L. Litov, E. Mihova, Z. Was, in preparation
41. P. Golonka, Photos+ - a C++ implementation of a universal Monte Carlo algorithm for QED radiative corrections in particle's decays, Master's thesis, Faculty of Nuclear Physics and Techniques, AGH University of Science and Technology, June, 1999; written under the supervision of Z. Was, available at http://cern.ch/Piotr.Golonka/MC/photos
42. M. Dobbs, J.B. Hansen, Comput. Phys. Commun. **134**, 41 (2001)